IEEE Access
Multidisciplinary | Rapid Review | Open Access Journal

Received January 12, 2019, accepted January 29, 2019, date of publication February 4, 2019, date of current version February 22, 2019.

Digital Object Identifier 10.1109/ACCESS.2019.2897170

Compact UWB-MIMO Antenna With High Isolation and Triple Band-Notched Characteristics

ZHIJUN TANG[1,2], XIAOFENG WU[2], JIE ZHAN[3], SHIGANG HU[2], ZAIFANG XI[2], AND YUNXIN LIU[3]

[1]School of Electronic Information and Electrical Engineering, Changsha University, Changsha 410022, China
[2]School of Information and Electrical Engineering, Hunan University of Science and Technology, Xiangtan 411201, China
[3]School of Physics and Electronic Science, Hunan University of Science and Technology, Xiangtan 411201, China

Corresponding authors: Xiaofeng Wu (xfwuvip@126.com) and Jie Zhan (jiezhanwl@163.com)

This work was supported in part by the National Natural Science Foundation of China under Grant 61875054, Grant 61675067, Grant 61674056, Grant 61575062, and Grant U1501253, in part by the Scientific Research Fund of the Hunan Provincial Education Department under Grant 16A072, and in part by the Science Research Fund Project of the Hunan University of Science and Technology under Grant KJ1812.

ABSTRACT A novel and high-performance four-element ultra-wideband (UWB) multiple-input multiple-output (MIMO) antenna is proposed in the paper. The proposed antenna is designed by using a novel integration technology of the symmetric layout, orthogonal structure, four-directional staircase-shaped decoupling, and multi-slit and multi-slot techniques. The mutual couplings among the antenna elements are significantly reduced by introducing the symmetric orthogonal and separated four-directional staircase-shaped structure. Furthermore, the antenna size is effectively miniaturized, and its impedance bandwidth is broadened by using a two-sided symmetric layout, partial and defected ground structure, the decoupling structure, and multi-slot and multi-slit techniques. Therefore, the antenna has the low-profile structure and a small dimension of 39mm×39mm×1.6mm. Moreover, the proposed antenna achieves triple band-notched characteristics by embedding different type slots and slits on the square radiating elements, default ground structure, and the decoupling structure, respectively. As a result, the antenna obtains the wider bandwidth of 2.30–13.75 GHz with the notched bands of 3.25–3.75 GHz, 5.08–5.90 GHz, and 7.06–7.95 GHz. The three notched bands are good in agreement with the existing interference bands of WiMAX (3.3–3.7 GHz), WLAN (5.15–5.875 GHz), and *X*-band (7.1–7.9 GHz), respectively. In addition, the proposed antenna also has a lower mutual coupling (<-22dB), lower envelop correlation coefficient (ECC<0.02, except for the three notched bands), high multiplexing efficiency ($\eta_{\mathrm{mux}} > -3.0$dB), stable gain, and quasi-omnidirectional radiation patterns at the entire impedance bandwidth. Therefore, a good tradeoff of the performance is obtained for the proposed antenna. The proposed antenna can be a good candidate for UWB-MIMO wireless communication applications, and especially for portable UWB-MIMO systems.

INDEX TERMS UWB-MIMO antenna, symmetric orthogonal structure, multi-slot-multi-slit, high isolation, triple band-notched characteristics.

I. INTRODUCTION

As the supplement of mobile communication network and wired network, various wireless access technologies have been developed rapidly in the past twenty years. In recent years, with the rise of Smart Home and Home Digital Entertainment Center, wireless access technology with 1Gb/s high transmission rate has attracted widespread attention. It has been confirmed that UWB-MIMO wireless communication system combining UWB technology with MIMO technology can achieve this goal. As we known, the main merits of the UWB wireless communication systems operating from 3.1 to 10.6GHz include high data rate [1], great capability to combat multipath fading, etc. Therefore, by combining the UWB wireless communication system with the MIMO technique, the multipath problem is treated as a favorable factor and the channel capability of the UWB communication system can be improved without additional bandwidth consumption, and thus a high data rate of 1Gb/s can be achieved in the UWB-MIMO communication system. Furthermore,

The associate editor coordinating the review of this manuscript and approving it for publication was Lu Guo.

the antenna is a key component of UWB-MIMO communication systems. Its performance directly affects the overall performance of the UWB-MIMO system. Therefore, the UWB-MIMO antenna has attracted extensive attentions and researches from many scholars [2]–[7].

At present, the researches on UWB-MIMO antennas mainly focus on miniaturization, broadband, high isolation and band-notched characteristics. The methods and techniques of antenna miniaturization mainly include meandering, high dielectric constant substrate, electro-magnetic band gap (EBG) [8], default ground structure (DGS) [9], symmetrical cutting half and loading reactance compensation, etc. The antenna band broadening technology mainly includes the gradual geometry structure, resonant structure and slot structure, etc. The methods to improve the isolation of antenna elements mainly include adding conductor branches, slotting, current neutralization [10], and diversity decoupling, etc. The band-notched characteristics of the antennas include embedding slots, loading structures, embedding branches, parasitic elements, split-ring resonators (SRR) and electromagnetic band gap (EBG) structures, etc. In [11], by using symmetrical cutting half technique, the UWB-MIMO antenna has a bandwidth from 3.1 GHz to more than 10.6 GHz with low mutual coupling and correlation. F-shaped stubs are introduced in the shared ground plane to reduce mutual coupling between the MIMO antenna elements in [12]. The rectangular band-notched design is realized in [13] by placing dual mushroom-type electromagnetic band gap (EBG) structures on the CPW feeding line. The relative high isolation and band-notched property are achieved in [14] by using two modified coplanar waveguides feeding staircase-shaped radiating elements for orthogonal radiation patterns and etching two split-ring resonator (SRR) slots on the radiators. In [15], the defected ground structure (DGS), closed-loop frequency selective surfaces and quad-strip connected circular are introduced to achieve high isolation. Based on meandering monopoles, the antenna achieves an ultra-wide bandwidth by involving two inverted L-shape parasitic strips and two smaller L-shape stubs, and a high isolation is obtained by etching a slot at the center of the ground in [16]. The MIMO antenna elements are placed orthogonally to achieve a good isolation between the two input ports, and half sized ground plane is used to reduce the size of the antenna [17]. A T-shaped stub is extruded in the ground plane to improve isolation and an L-shaped stub to introduce band-notched function in [18]. A complementary split-ring resonator (CSRR) is incorporated into the patch to achieve the dual notched band characteristics in [19]. In order to enhance isolation, [20] uses a rectangular ground plane with an extruded T-shaped stub. In [21], the antenna design employs a hybrid isolation enhancing (inverted-L stubs) and miniaturization technique (CSRR). Miniaturization and high isolation are achieved by using a combination of techniques in [22]. The tapered microstrip fed slot antenna acts as a single radiating element with inverted L-shaped slits to introduce two notches in [23]. Decoupling structures are presented in the top and bottom layers of the substrate in [24]. However, there is always a trade-off of antenna size, bandwidth, radiation pattern, isolation, band-notched characteristics, and complexity in all of these reported methods and techniques. Therefore, the good trade-off of the performance for UWB-MIMO antenna design is a challenging task. In addition, most of the designs in the published literatures focus on single band-rejection feature of two elements UWB-MIMO antennas, and the four-element UWB-MIMO antenna with multiple band-notched characteristics is rarely reported.

In this paper, based on some related literatures [6], [7], [24]–[28], a novel four-element UWB-MIMO antenna is presented to operate in the UWB band range with the band-rejected ability to operate at 3.3-3.7GHz (WiMAX band), 5.15-5.875GHz (WLAN band), and 7.1-7.9GHz (X-band) respectively. The four elements of the proposed antenna are identical, and they are symmetrically and orthogonally distributed on both sides of the substrate. Each element of the antenna consists of a square patch and a rectangular default ground plane. Four separated and mutually adjacent-orthogonal staircase-shaped patches are used to reduce the mutual coupling among the radiating elements. Furthermore, multiple notched bands are obtained by embedding different slots and slits on the antenna elements. The simulated and measured results confirm that the proposed UWB-MIMO antenna has a wider impedance bandwidth, stable gain, quasi-omnidirectional radiation patterns and higher isolation. It is clearly shows that the proposed antenna obtains a good trade-off of the performance.

II. ANTENNA DESIGN AND ANALYSIS

The geometry structure and layout with parameters of the antenna is shown in Fig. 1. Design and development of the proposed antenna has been carried out by using parametric analysis and optimization in CST STUDIO SUITE. The design process of the antenna is described as follows.

A. ULTRA-WIDEBAND DESIGN

The design steps of the antenna, including antenna (a), (b) and (c), are shown in Fig. 2-Fig. 4 respectively. Initially, each element of the antenna consists of a square-shaped patch fed by a microstrip line and a rectangular defected ground plane, which is illustrated in Fig. 2. To broaden the bandwidth of the antenna at the higher frequency bands, a small rectangular slit is etched in the defected ground plane. Two elements (element 1 and 3) are laid on the top layer of the substrate, and the other two elements (element 2 and 4) are laid on the bottom layer of the substrate. Furthermore, element 1 and 3 are orthogonal to the element 2 and 4, respectively. In other words, these adjacent elements are orthogonal to each other, which can reduce the mutual couplings between the adjacent elements. Furthermore, the bandwidth of the antenna can also be broadened by introducing decoupling elements, multiple type slots and slits, which are demonstrated in the section of S-parameters analysis.

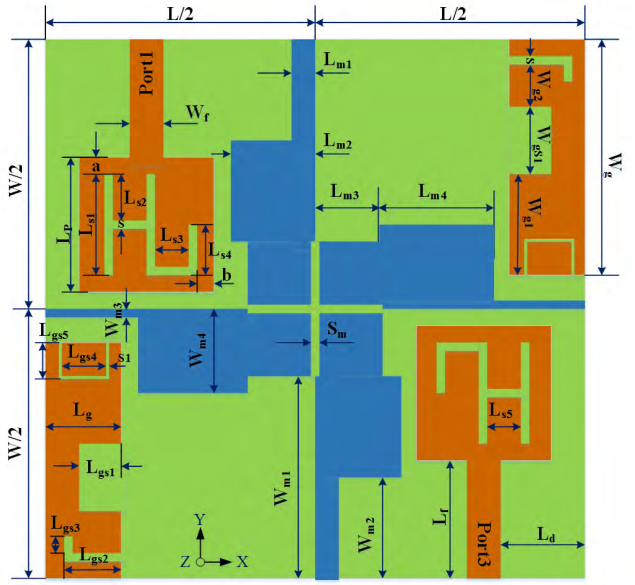

FIGURE 1. The proposed antenna structure with geometry parameters.

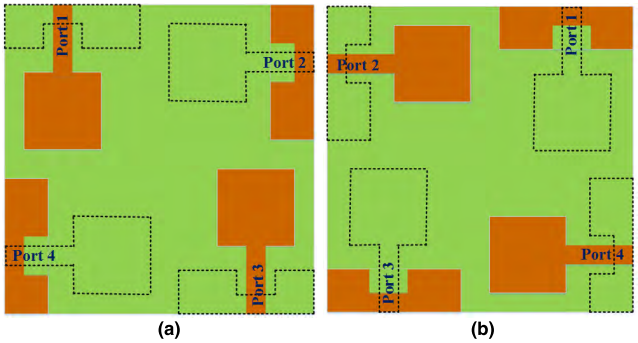

FIGURE 2. The antenna (a) layout for ultra wideband and multiple ports. (a) Top view (b). Back view.

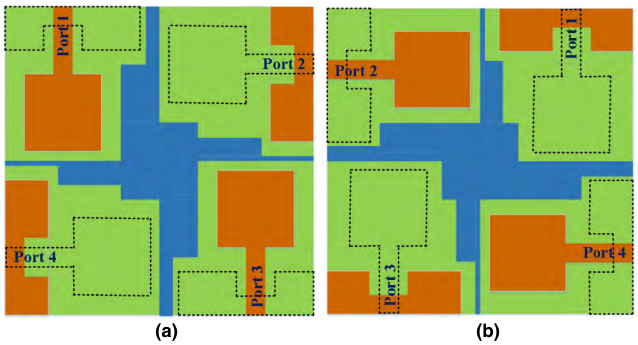

FIGURE 3. The antenna (b) layout with initial decoupling structure. (a) Top view. (b) Back view.

B. DECOUPLING STRUCTURE DESIGN

Firstly, in order to reduce the mutual coupling among the elements of the UWB-MIMO antenna, the adjacent elements are designed to be orthogonal to each other, as described in the UWB design section. Secondly, in order to further reduce the mutual couplings, two identical and symmetric four-directional staircase-shaped radiating patches are added to the centre of top layer and bottom layer of the antenna, respectively. The preliminary decoupling structure is show in Fig. 3. According to S-parameters analysis results, the initial decoupling structure performs well in high frequency band, but there are still some shortcomings in low frequency band. The improved decoupling structure is shown in Fig. 4.

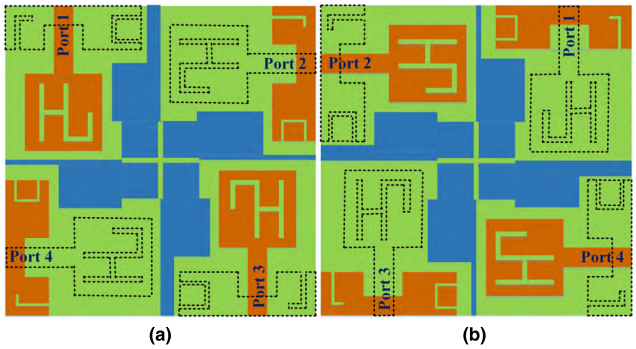

FIGURE 4. The antenna (c) layout with three notched bands and the improved decoupling structure. (a) Top view. (b) Back view.

C. MULTIPLE NOTCHED BANDS DESIGN

In order to realize multiple band-notched characteristics, the antenna structure need to be further designed. In recent years, various techniques have been studied to generate band-notched characteristics [29]–[33], among which the slot and slit techniques are considered to be effective methods to generate notches [1], [23], [34]–[39]. Therefore, an H-L-shaped slot is embedded on the square radiating patch for generating a notched band accord with WLAN operating band. Furthermore, a small L-shaped slit and a U-shaped slit are etched in the defected ground plane for generating two notched bands accord with X-band operating frequencies and WiMAX band respectively. Furthermore, in order to further reduce mutual coupling, i.e. increase isolation, the initial staircase-shaped decoupling structure is split by using two mutually orthogonal slots. As a result, the improved decoupling structure consists of four small mutually orthogonal staircase-shaped patches, which can reduce interference between itself. The antenna layout with three band-notched characteristics is illustrated in Fig. 4.

In order to demonstrate that the antenna can generate these notches, the surface currents of the antenna are analyzed. The effects of the U-shaped slit, the H-L-shaped slot and the L-slit can also be verified by plotting the surface currents at (a) 3.5 GHz (b) 5.5 GHz (c) 7.5GHz to achieve band-rejection as illustrated in Fig. 5. It is clear that surface currents are mainly concentrated on the U-shaped slit, the H-L-shaped slot and the L-slit at 3.5GHz, 5.5 GHz and 7.5GHz respectively. The surface currents along the slots or slits are in opposite directions on top and bottom sides for the three cases. As a result, radiation from one side currents will be cancelled by the other side currents. Hence, no radiation or

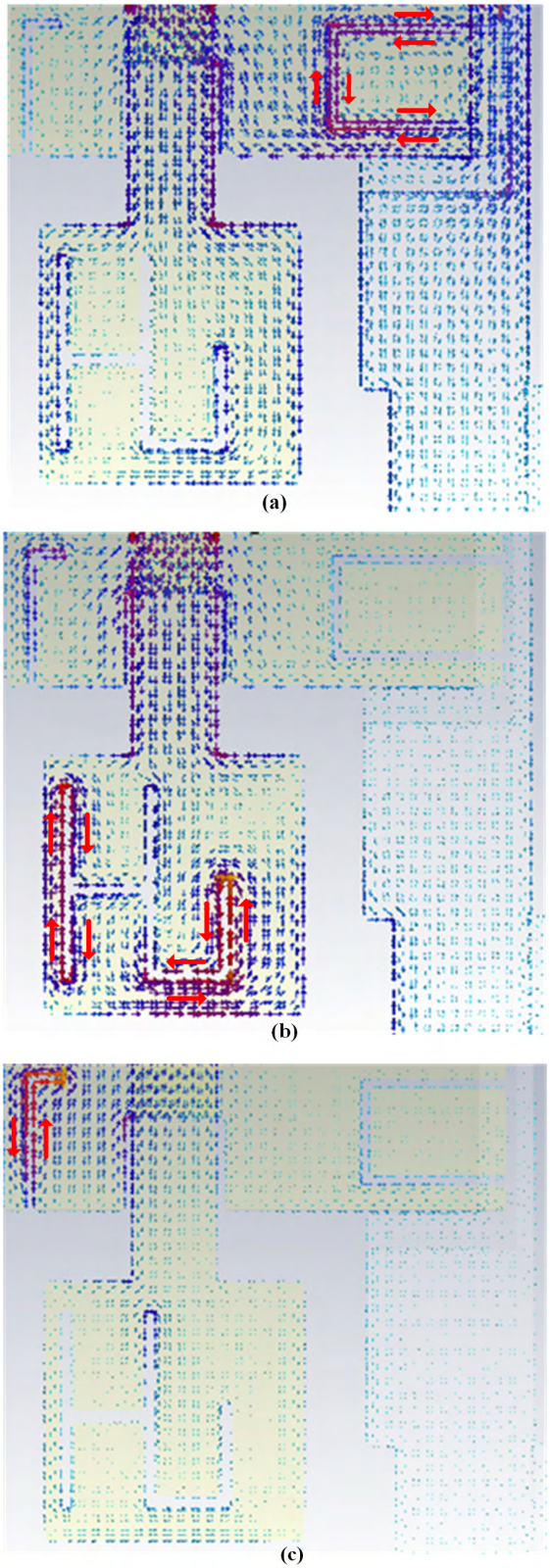

FIGURE 5. The surface current distribution of the proposed antenna when the port 1 is excited at: (a)3.5GHz, (b) 5.5GHz,(c) 7.5GHz.

very low radiation occurs, and thus return loss of the antenna is larger. Furthermore, it is also observed that the improved decoupling structure is beneficial to generating the WiMAX

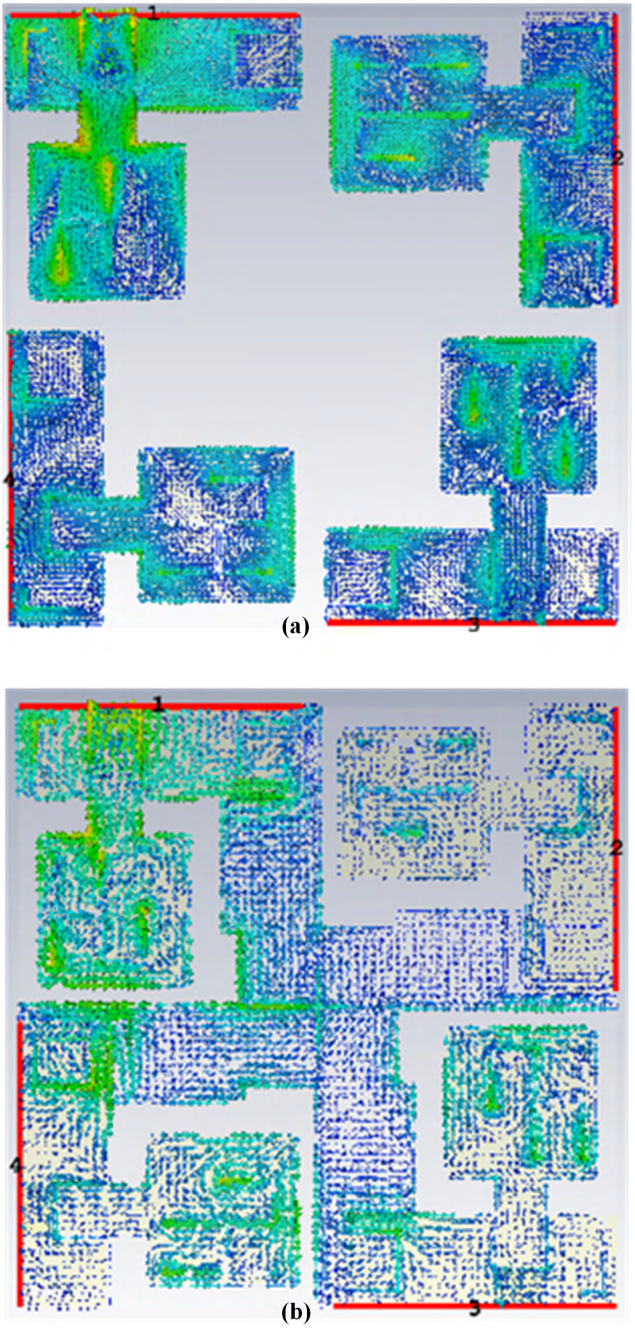

FIGURE 6. The surface current distribution of the proposed antenna when the port 1 is excited at 9.5 GHz: (a) without decoupling structure, (b) with decoupling structure.

band-rejection as shown in Fig. 5 (a). These results show that the antenna can effectively achieve triple notches at the WiMAX, WLAN and X-band operating frequency band respectively. The band-notched characteristics are further confirmed in the following section of S-parameters analysis.

To demonstrate the decoupling effects of the four mutually orthogonal staircase-shaped patches, the surface current distributions of the proposed antenna are depicted in Fig. 6 when the port 1 is excited at 9.5 GHz. From in

Fig. 6(a) and Fig. 6(b), it is clearly observed that the mutual couplings among the elements of the antenna without the decoupling structure are much stronger than those of the antenna with the decoupling structure. The result is also further confirmed in the section of S-parameters analysis.

D. S-PARAMETERS ANALYSIS

Optimized design parameters of the proposed antenna with three notched bands are shown in Tab.1. Considering that four elements of the antenna are identical, for simplicity, the performance of the antenna is analyzed by taking one element as the representative. Without loss of generality, the S-parameters of the element 1 (Port 1) are analyzed for the antenna design in the following section.

Return loss (S11) of the antenna is shown in Fig. 7. It is can be noticed from Fig. 7 that the antenna (a) has the bandwidth of 2.02-10.70GHz, which can cover the entire UWB band of 3.1-10.6GHz. The antenna (b) has the bandwidth of 2.26-10.65GHz. The antenna (c) obtains the bandwidth of 2.35-14.0GHz with three notched bands of 3.28-3.80GHz, 5.10-5.88GHz and 7.09-7.92GHz. As a result, compared with antenna (a), the impedance bandwidth of the antenna (b) is almost unchanged by introducing initial decoupling structure of four-directional staircase-shaped radiating patches. Furthermore, the desired triple band-notched characteristics are obtained by embedding slots and slits on the antenna (c) and splitting the initial staircase-shaped patches into four small sections. Compared with the antenna (a) and (b), impedance bandwidth of the antenna (c) is broadened by improving the antenna structure.

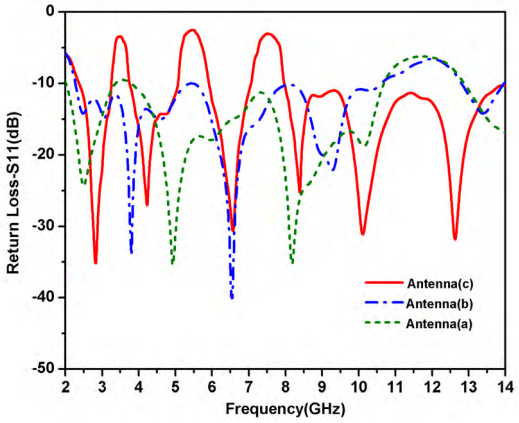

FIGURE 7. The return loss of Port 1 for the three antennas.

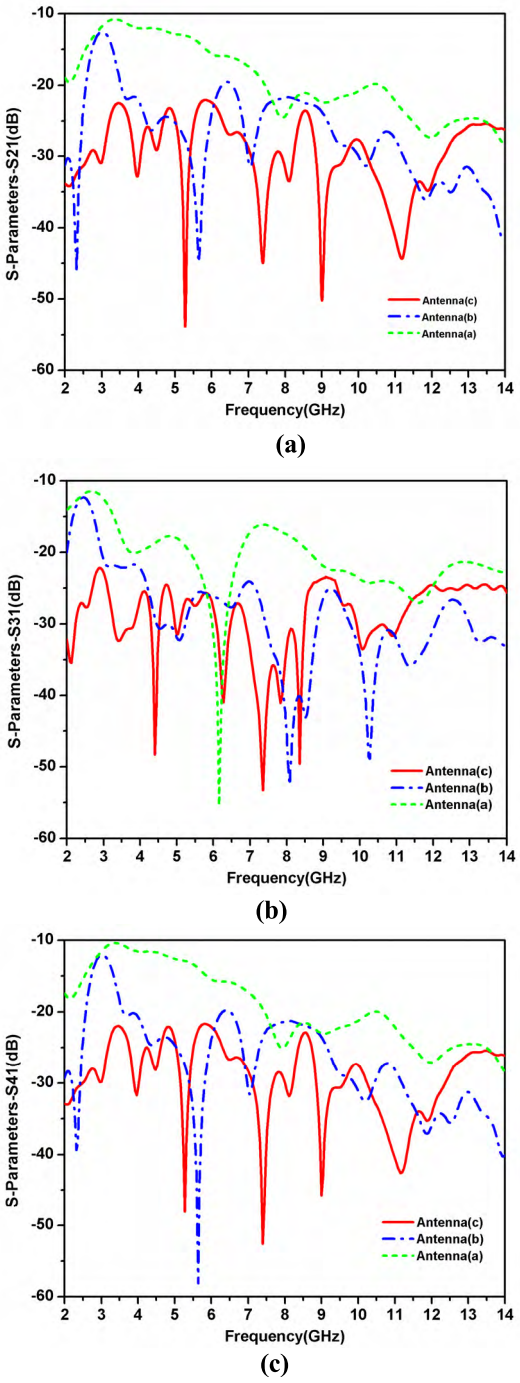

FIGURE 8. S-parameters of the three antennas: (a)S21, (b)S31, (c)S41.

S-Parameters S21, S31 and S41 of the three antennas are illustrated in Fig. 8 (a)-(c), respectively. Due to structural symmetry, S21 and S41 are almost identical. Compared with S21 and S41, S31 is smaller for the reason of the farther distance between port 1 and port 3 than that of port 1 and port 2 or port 4.

It can be also observed that the antenna (a) without decoupling structure has large value of S21, S31 and S41, which show larger mutual couplings among the different ports of the antenna (a). The antenna (b) with the four-directional staircase-shaped decoupling structures has small value of S21, S31 and S41 except for the lower frequency band. Moreover, for the antenna (b), S21 is larger than −20dB at 2.60-3.52GHz, S41 is larger than −20dB at 2.60-3.60GHz, and S31 is larger than −20dB at 2.03-2.92GHz. The analysis results of these S-parameters indicate that the decoupling structure of the proposed antenna need to be further improved. Therefore, by splitting the four-directional staircase-shaped decoupling structure with two

small mutually orthogonal slots, the antenna (c) has smaller values of S21, S31 and S41, all of which are less than −20dB at the entire operating band.

III. RESULTS AND DISSCUSIONS

The proposed UWB-MIMO antenna is printed on a low cost FR4 substrate with the dielectric permittivity of ε_r=4.4 and loss tangent $tan\delta$=0.025. The dimension of the antenna is 39mm×39mm×1.6mm. S-parameters, gain, radiation patterns, and MIMO diversity were measured by the Agilent vector network analyzer for the proposed antenna. The simulations of the antenna were carried out by using the CST Microwave Studio.

A. S-PARAMETERS

Return loss is a key parameter for characterizing the operating bands of the antenna. The simulated and measured results of return loss (S11) are shown in Fig. 9. It can be observed from Fig. 9 that the proposed antenna achieves wider bandwidth of 2.30-13.75GHz with three notched bands of 3.25-3.75GHz, 5.08-5.90GHz and 7.06-7.95GHz. The three notched bands are good in agreement with the bands of WiMAX (3.3-3.7GHz), WLAN (5.15-5.875GHz) and X-band (7.1-7.9GHz), respectively. Furthermore, the measured results are consistent with the simulated results at low frequency bands, and some small fluctuations between the measured and simulated results at the higher frequency bands. This phenomenon can be attributed to the fact that the measured and fabricated limitations are more susceptible to the higher frequencies. As a while, the measured values of return loss are good in agreement with the simulated values.

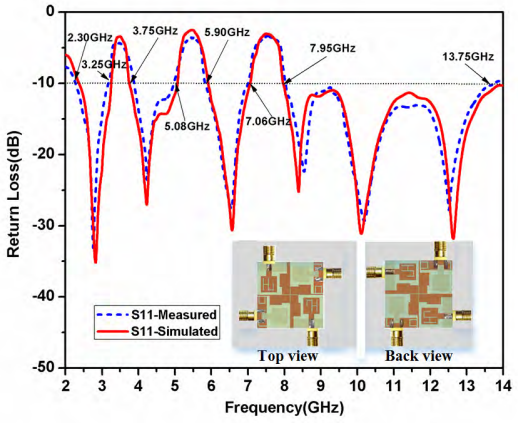

FIGURE 9. Simulated and measured results of S11-parameters.

In addition, the S-parameters S21, S31, and S41 are important parameters for describing the isolation of the UWB-MIMO antenna. The measured and simulated results of S21, S31, and S41 are shown in Fig. 10. It can be observed that the values of S21, S31, and S41 are all less than −22dB at entire operating frequency band. The values of S21 and S41 are almost identical owing to the symmetrical structure of the proposed antenna, which are consistent with the results

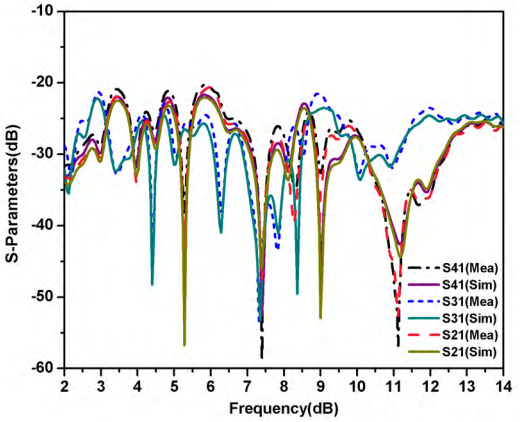

FIGURE 10. Simulated and measured results of S21, S31, and S41.

of the section II D. Furthermore, the measured values of S21, S31, and S41 are good in agreement with the simulated values. These results show the UWB-MIMO antenna has higher isolation.

B. THE GAIN AND RADIATION PATTERNS

The antenna gain is also an important parameter for describing the degree of concentration and enlargement of an input power. It is used to measure the ability of antenna to send and receive signals in a specific direction. Therefore, antenna gain is also related to its radiation characteristics. The measured and simulated results of the peak gain are shown in Fig. 11. It can be observed that the measured peak gains are consistent with the simulated results. For the impedance bandwidth of 2.30-13.75GHz, the peak gain changes from 1.40dBi to 4.60dBi at high frequency band (4.0-13.75GHz) except for the notched bands. In addition, the peak gain is small at lower frequencies (2.3-4.0GHz) for the reason of small size for one element. However, the peak gain is significantly increased because the excitation and radiation modes of higher order modes become partially oriented at higher frequencies (6.0-13.75GHz). Although the variation

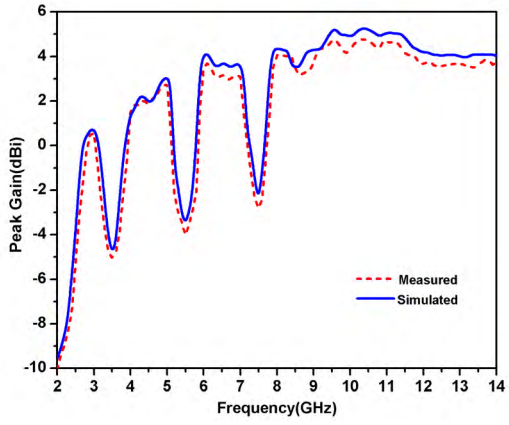

FIGURE 11. Simulated and measured peak gain of the proposed antenna.

of the peak gain is about 3.20dBi, it is acceptable considering the wider bandwidth for the proposed UWB-MIMO antenna.

The Fig. 12 shows the simulated and measured radiation patterns in E-plane and H-plane for the antenna at sample frequencies of 4, 7 and 10GHz respectively. It is observed form Fig. 12 that the E-plane radiation characteristics of high frequencies are almost the same as those of the low frequencies. The E-plane co-polarizations of the three sample frequencies have two main beams in the broadside direction (−75°, 80°) and (105°, 260°), and the cross-polarizations are small. Furthermore, the differences between the co-polarizations and the cross-polarizations in the broadside direction are larger than 15.0dB, which shows good radiation patterns in E-plane. It can be also observed in Fig. 12 that the co-polarizations in H-plane are quasi-omnidirectional and the cross-polarizations are all smaller for the three samples frequencies. Moreover, the differences between the co-polarizations and the cross-polarizations are larger than 20.0dB, which exhibits the stable radiation patterns in H-plane. The measured radiation patterns are good in agreement with the simulated values.

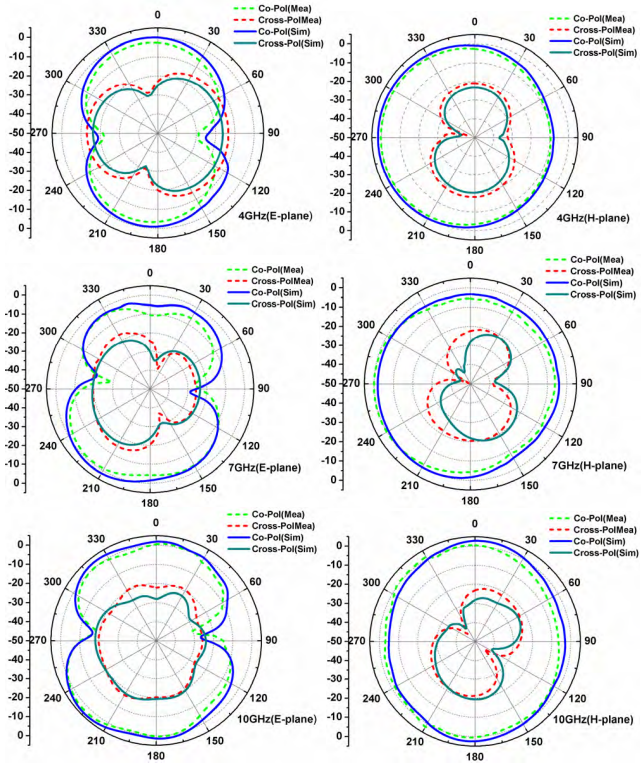

FIGURE 12. Simulated and measured radiation patterns of the proposed antenna in E-plane and H-plane.

C. DIVERSITY CHARACTERISTICS

Envelop correlation coefficient(ECC), diversity gain(DG), multiplexing efficiency(ME), channel capacity loss(CCL) and total active reflection coefficient(TARC) are important parameters for validating the capability and performance of

TABLE 1. Dimensions of optimized parameters for the proposed antenna.

Parameters	Dimension(mm)	Parameters	Dimension(mm)
L (W)	39.0	L_{s2}	3.7
L_p	9.5	L_{s3}	2.3
L_f	8.5	L_{s4}	4.0
W_f	3.0	L_{s5}	2.6
L_g	5.8	L_{gs1}	3.0
W_g	18.5	L_{gs2}	5.1
L_d	5.3	L_{gs3}	1.5
L_{m1}	2.0	L_{gs4}	3.4
L_{m2}	6.1	L_{gs5}	4.4
L_{m3}	5.0	W_{g1}	9.8
L_{m4}	7.2	W_{g2}	3.7
W_{m1}	14.5	W_{gs1}	3.8
W_{m2}	7.0	W_{m3}	0.6
L_{s1}	7.4	W_{m4}	6.1
a	1.0	h	1.6
b	2.5	S	0.5
S1	0.4	S_m	0.2

MIMO antennas. ECC is used to characterize the correlation among antenna elements. In order to achieve higher diversity among MIMO antenna elements, ECC should be lower. The acceptable range of ECC is less than 0.5. For multi-port MIMO antennas, the envelope correlation coefficient (ECC) ρ_{eij}, using simulated 3-D radiation patterns was numerically calculated by using the following equation [4], [21], [40], [41]. where i and j are port number, XPR is the cross-polarization ratio, P_θ and P_φ are the $\theta$and φcomponents of the angular density functions of the incoming wave. The diversity gain (DG) of MIMO antennas can be calculated by the following equation.

$$DG = 10\sqrt{1 - ECC^2} \tag{2}$$

The multiplexing efficiency (η_{mux}) is calculated by the following equation [12], [42].

$$\eta_{mux} = \sqrt{\eta_i \eta_j (1 - |\rho_c|^2)} \tag{3}$$

where η_i is the total efficiency of the ithantenna element, ρ_c is the magnitude of the complex correlation between the ith and jth antenna elements, and $|\rho_c|^2 \approx ECC$.

The ECC and DG of the proposed UWB-MIMO antenna is illustrated in Fig. 13. It can be observed that the ECC is very smaller (<0.02) at entire impedance bandwidth except the above-mentioned notched bands. Although the ECC is influenced by these notches, it is less than 0.05 at entire impedance bandwidth. Furthermore, The DG of the antenna is larger than 9.5dBi at entire impedance bandwidth except for the three notched bands. It reveals that the proposed antenna has the smaller ECC and the larger DG.

The multiplexing efficiency and peak gain of the antenna are described in Fig. 14. It is observed that the multiplexing efficiency and peak gain both have triple band-notched characteristics, which are consistent with the previous analysis

TABLE 2. Performance comparisons with the previous published literatures.

Published literature	Antenna size(mm^2)	Bandwidth (GHz)	Gain(dBi)	Isolation (dB)	ECC	CCL (bps/Hz)	TARC (dB)	Notched band	Port number	Size/port (mm^2)
Ref.[21]	23×29	3-12	1.2-5.9	>15	<0.15	NA	NA	NA	2	333.5
Ref.[3]	50×40	2.7-12.0	2.0-5.7	>17	<0.03	NA	NA	1	4	500
Ref.[12]	50×30	2.5-14.5	0.1-4.0	>20	<0.04	NA	NA	NA	2	750
Ref.[4]	30×30	3.1-11.0	2.0-5.0	>20	<0.02	<0.35	<-10	1	2	450
Ref.[23]	34×18	2.93-20.0	0-7.0	>22	<0.01	NA	<-20	2	2	306
Ref.[8]	64×45	2.5-11.0	0-6.0	>15	<0.02	NA	NA	3	2	1440
Ref.[24]	40×40	3.1-11	1.3-4.0	>20	<0.01	<0.4	NA	NA	4	400
Ref.[25]	40×26	2.9-10.6 2.9-12.0	0.9-6.5	>15	<0.2	NA	NA	NA	2	520
Ref.[26]	38×38	3.0-15.0	0.5-5.0	>15	<0.15	<0.4	NA	NA	4	361
Ref.[6]	35×35	3.0-12.0	NA	>20	<0.3	NA	NA	1	4	306.3
Ref.[7]	45×45	2.0-10.6	1.5-4.5	>17	<0.01	<0.4	NA	1	4	506.3
Ref.[27]	50×39.8	2.7-12.0	2.5-6.0	>17	NA	NA	NA	1	4	497.5
Ref.[28]	35×35	3.0-12.0	3.0 stable	>15	<0.07	NA	NA	NA	4	306.3
The work	39×39	2.3-13.75	1.4-4.6	>22	<0.02	<0.2	<-10	3	4	380.3

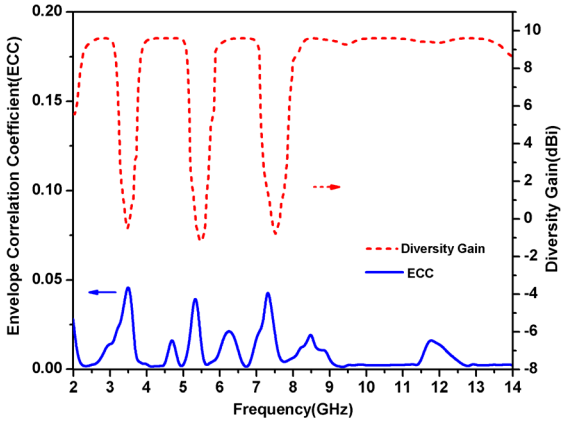

FIGURE 13. The ECC and DG of the proposed antenna.

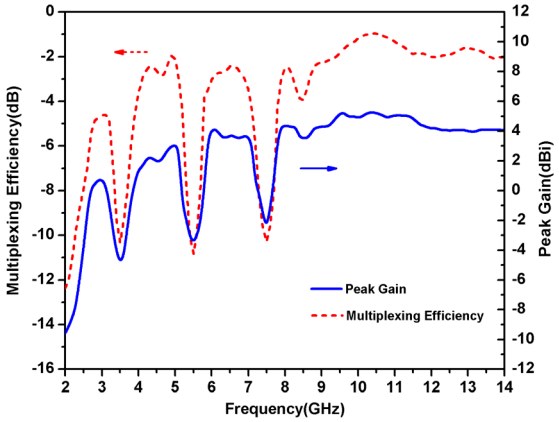

FIGURE 14. The multiplexing efficiency and peak gain of the proposed antenna.

results. Furthermore, for the entire impedance bandwidth (2.30-13.75GHz) except for three notched bands, the multiplexing efficiency is larger than −3dB at 4.0-13.75GHz and it decrease to −3dB only at the lower narrow frequency band (2.3-4.0GHz), which reveals the UWB-MIMO antenna has high multiplexing efficiency.

In general, the channel capacity of the MIMO system varies linearly with increasing number of used antenna elements. However, it also includes some losses due to the presence of correlation among the MIMO channels. The correlation among elements in MIMO channel systems produces capacity loss. Therefore, the CCL is an essential parameter to characterize the channel capacity of the MIMO system. The CCL of the antenna is depicted in Fig. 15. For MIMO system, the desired value of the CCL is less than 0.4bps/Hz. It is observed that except for the three notched bands, the CCLs of the antenna are less than 0.2bps/Hz over the entire band. It shows that the antenna has a good diversity performance.

The TARC is defined as the square root of the ratio of total reflected power to the total incident power and apparent return loss of the overall MIMO antenna system [20]. For the MIMO system, the desired value of the CCL is less than 0dB. The TARC of the antenna is depicted in Fig. 15. It is shown in Fig. 15 that the TARC is less than −10dB for the entire band except for the three notched bands.

D. PERFORMANCE COMPARISON

Table 2 shows a comparison of the proposed antenna with some representative UWB-MIMO antennas published in

$$\rho_{eij} = \frac{\left|\int_0^{2\pi}\int_0^{\pi}\left(XPR\cdot E_{\theta i}\cdot E_{\theta j}^{*}\cdot P_{\theta}+E_{\varphi i}\cdot E_{\varphi j}^{*}\cdot P_{\varphi}\right)d\Omega\right|^{2}}{\int_0^{2\pi}\int_0^{\pi}\left(XPR\cdot E_{\theta i}\cdot E_{\theta i}^{*}\cdot P_{\theta}+E_{\varphi i}\cdot E_{\varphi i}^{*}\cdot P_{\varphi}\right)d\Omega\times\int_0^{2\pi}\int_0^{\pi}\left(XPR\cdot E_{\theta j}\cdot E_{\theta j}^{*}\cdot P_{\theta}+E_{\varphi j}\cdot E_{\varphi j}^{*}\cdot P_{\varphi}\right)d\Omega} \quad (1)$$

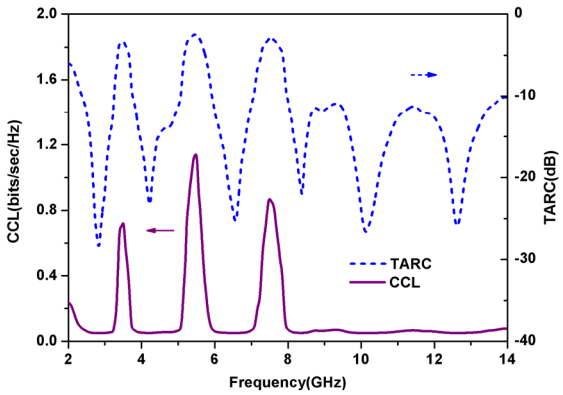

FIGURE 15. The CCL and TARC of the proposed antenna.

recent years. The definition of ''Size/port'' in the Tab.2 is used for describing the size of each element. Although the comparison is not comprehensive, it almost represents the current state-of-the-art of UWB-MIMO technology. It is confirmed from the comparison results that the proposed antenna achieves a good trade-off of the size, bandwidth, gain, radiation pattern, isolation, MIMO diversity (ECC, DG, ME, CCL and TARC), band-notched characteristics and the number of elements.

IV. CONCLUSION

A compact four-element UWB-MIMO antenna is presented in this paper. Miniaturization and high performance are achieved by introducing an organic integration of the symmetric layout, orthogonal structure, separated four-directional staircase-shaped decoupling, multi-slot and multi-slit techniques. Moreover, some key parameters, such as S-parameters, gain, radiation patterns, isolation and MIMO diversity, are investigated by simulating and measuring. The measured and simulated results are good in agreement with each other. These results confirm that the proposed UWB-MIMO antenna achieves the wider impedance bandwidth with multiple band-notched characteristics, stable gain, quasi-omnidirectional radiation patterns, higher isolation and good diversity properties, which reveal a good trade-off of the performance for the antenna. Therefore, the proposed antenna can be a good candidate for UWB-MIMO wireless communication applications, and especially a potential candidate for portable UWB-MIMO systems.

REFERENCES

[1] Z. Tang, X. Wu, J. Zhan, Z. Xi, and S. Hu, ''A novel miniaturized antenna with multiple band-notched characteristics for UWB communication applications,'' *J. Electromagn. Waves Appl.*, vol. 32, no. 15, pp. 1961–1972, Jun. 2018.

[2] X. Zhao, S. P. Yeo, and L. C. Ong, ''Planar UWB MIMO antenna with pattern diversity and isolation improvement for mobile platform based on the theory of characteristic modes,'' *IEEE Trans. Antennas Propag.*, vol. 66, no. 1, pp. 420–425, Jan. 2018.

[3] S. M. Khan, A. Iftikhar, S. M. Asif, A.-D. Capobianco, and B. D. Braaten, ''A compact four elements UWB MIMO antenna with on-demand WLAN rejection,'' *Microw. Opt. Technol. Lett.*, vol. 58, no. 2, pp. 270–276, Feb. 2016.

[4] S. P. Biswal and S. Das, ''A low-profile dual port UWB-MIMO/diversity antenna with band rejection ability,'' *Int. J. RF. Microw. Comput.-Aided Eng.*, vol. 28, no. 1, Jan. 2017, Art. no. e21159.

[5] Y.-Y. Liu and Z.-H. Tu, ''Compact differential band-notched stepped-slot UWB-MIMO antenna with common-mode suppression,'' *IEEE Antennas Wireless Propag. Lett.*, vol. 16, pp. 593–595, 2017.

[6] J. Zhu, S. Li, B. Feng, L. Deng, and S. Yin, ''Compact dual-polarized UWB quasi-self-complementary MIMO/diversity antenna with band-rejection capability,'' *IEEE Antennas Wireless Propag. Lett.*, vol. 15, pp. 905–908, 2016.

[7] S. Tripathi, A. Mohan, and S. Yadav, ''A compact koch fractal UWB MIMO antenna with WLAN band-rejection,'' *IEEE Antennas Wireless Propag. Lett.*, vol. 14, pp. 1565–1568, 2015.

[8] N. Jaglan, S. D. Gupta, E. Thakur, D. Kumar, B. K. Kanaujia, and S. Srivastava, ''Triple band notched mushroom and uniplanar EBG structures based UWB MIMO/diversity antenna with enhanced wide band isolation,'' *AEU-Int. J. Electron. Commun.*, vol. 90, pp. 36–44, Jun. 2018.

[9] C.-M. Luo, J.-S. Hong, and L.-L. Zhong, ''Isolation enhancement of a very compact UWB-MIMO slot antenna with two defected ground structures,'' *IEEE Antennas Wireless Propag. Lett.*, vol. 14, pp. 1766–1769, 2015.

[10] S. Zhang and G. F. Pedersen, ''Mutual coupling reduction for UWB MIMO antennas with a wideband neutralization line,'' *IEEE Antennas Wireless Propag. Lett.*, vol. 15, pp. 166–169, 2016.

[11] L. Liu, S. W. Cheung, and T. I. Yuk, ''Compact multiple-input–multiple-output antenna using quasi-self-complementary antenna structures for ultrawideband applications,'' *IET Microw., Antennas Propag.*, vol. 8, no. 13, pp. 1021–1029, Oct. 2014.

[12] A. Iqbal, O. A. Saraereh, A. W. Ahmad, and S. Bashir, ''Mutual coupling reduction using F-shaped stubs in UWB-MIMO antenna,'' *IEEE Access*, vol. 6, pp. 2755–2799, 2018.

[13] L. Peng, B.-J. Wen, X.-F. Li, X. Jiang, and S.-M. Li, ''CPW fed UWB antenna by EBGs with wide rectangular notched-band,'' *IEEE Access*, vol. 4, pp. 9545–9552, 2016.

[14] P. Gao, S. He, X. Wei, Z. Xu, N. Wang, and Y. Zheng, ''Compact printed UWB diversity slot antenna with 5.5-GHz band-notched characteristics,'' *IEEE Antenna Wireless Propag. Lett.*, vol. 13, pp. 376–379, 2014.

[15] R. Saleem, M. Bilal, K. B. Bajwa, and M. F. Shafique, ''Eight-element UWB-MIMO array with three distinct isolation mechanisms,'' *Electron. Lett.*, vol. 51, no. 4, pp. 311–313, Feb. 2015.

[16] J.-Y. Deng, L.-X. Guo, and X.-L. Liu, ''An ultrawideband MIMO antenna with a high isolation,'' *IEEE Antenna Wireless Propag. Lett.*, vol. 15, pp. 182–185, 2016.

[17] A. Toktas and A. Akdagli, ''Compact multiple-input multiple-output antenna with low correlation for ultra-wide-band applications,'' *IET Microw., Antennas Propag.*, vol. 9, no. 8, pp. 822–829, Jun. 2015.

[18] R. Chandel and A. K. Gautam, ''Compact MIMO/diversity slot antenna for UWB applications with band-notched characteristic,'' *Electron. Lett.*, vol. 52, no. 5, pp. 336–338, Mar. 2016.

[19] W. T. Li, Y. Q. Hei, H. Subbaraman, X. W. Shi, and R. T. Chen, ''Novel printed filtenna with dual notches and good out-of-band characteristics for UWB-MIMO applications,'' *IEEE Microw. Wireless Compon. Lett.*, vol. 26, no. 10, pp. 765–767, Oct. 2016.

[20] R. Chandel, A. K. Gautam, and K. Rambabu, ''Design and packaging of an eye-shaped multiple-input–multiple-output antenna with high isolation for wireless UWB applications,'' *IEEE Trans. Compon., Packag. Manuf. Technol.*, vol. 8, no. 4, pp. 635–642, Apr. 2018.

[21] M. S. Khan, A.-D. Capobianco, S. M. Asif, D. E. Anagnostou, R. M. Shubair, and B. D. Braaten, ''A compact CSRR-enabled UWB diversity antenna,'' *IEEE Antenna Wireless Propag. Lett.*, vol. 16, pp. 808–812, 2016.

[22] M. S. Khan, A.-D. Capobianco, A. Iftikhar, R. M. Shubair, D. E. Anagnostou, and B. D. Braaten, ''Ultra-compact dual-polarised UWB MIMO antenna with meandered feeding lines,'' *IET Microw., Antennas Propag.*, vol. 11, no. 7, pp. 997–1002, Jun. 2017.

[23] R. Chandel, A. K. Gautam, and K. Rambabu, ''Tapered fed compact UWB MIMO-diversity antenna with dual band-notched characteristics,'' *IEEE Trans. Antennas Propag.*, vol. 66, no. 4, pp. 1677–1684, Apr. 2018.

[24] W. A. E. Ali and A. A. Ibrahim, ''A compact double-sided MIMO antenna with an improved isolation for UWB applications,'' *AEU-Int. J. Electron. Commun.*, vol. 82, pp. 7–13, Dec. 2017.

[25] L. Liu, S. W. Cheung, and T. I. Yuk, ''Compact MIMO antenna for portable devices in UWB applications,'' *IEEE Trans. Antennas Propag.*, vol. 61, no. 8, pp. 4257–4264, Aug. 2013.

[26] D. Sipal, M. P. Abegaonkar, and S. K. Koul, "Easily extendable compact planar UWB MIMO antenna array," *IEEE Antennas Wireless Propag. Lett.*, vol. 16, pp. 2328–2331, 2017.
[27] M. S. Khan, A. D. Capobianco, S. Asif, A. Iftikhar, B. Ijaz, and B. D. Braaten, "Compact 4×4 UWB-MIMO antenna with WLAN band rejected operation," *Electron. Lett.*, vol. 51, no. 14, pp. 1048–1050, Jul. 2015.
[28] Z. Wani and D. Kumar, "A compact 4×4 MIMO antenna for UWB applications," *Microw. Opt. Technol. Lett.*, vol. 58, no. 6, pp. 1433–1436, Jun. 2016.
[29] J. Wang, Y. Yin, and X. Liu, "A novel compact planar ultra-wideband antenna with dual band-notched characteristics," *Int. J. RF Microw. Comput.-Aided Eng.*, vol. 25, no. 1, pp. 48–55, Jan. 2015.
[30] W. Wu, B. Yuan, and A. Wu, "A quad-element UWB-MIMO antenna with band-notch and reduced mutual coupling based on EBG structures," *Int. J. Antennas Propag.*, vol. 2018, Feb. 2018, Art. no. 8490740.
[31] T.-C. Tang and K.-H. Lin, "An ultrawideband MIMO antenna with dual band-notched function," *IEEE Antennas Wireless Propag. Lett.*, vol. 13, pp. 1076–1079, 2014.
[32] J.-F. Li, Q.-X. Chu, Z.-H. Li, and X.-X. Xia, "Compact dual band-notched UWB MIMO antenna with high isolation," *IEEE Trans. Antennas Propag.*, vol. 61, no. 9, pp. 4759–4766, Sep. 2013.
[33] D. Yadav, M. P. Abegaonkar, S. K. Koul, V. N. Tiwari, and D. Bhatnagar, "Two element band-notched UWB MIMO antenna with high and uniform isolation," *Prog. Electromagn. Res. M*, vol. 63, pp. 119–129, 2018.
[34] Z.-J. Tang, J. Zhan, Z.-F. Xi, S.-G. Wu, and M. Li, "A compact triple band-notched UWB printed antenna with multistep patches integrated by multitype slots," *Microw. Opt. Technol. Lett.*, vol. 59, no. 2, pp. 270–275, Feb. 2017.
[35] S. R. Emadian and J. Ahmadi-Shokouh, "Very small dual band-notched rectangular slot antenna with enhanced impedance bandwidth," *IEEE Trans. Antennas Propag.*, vol. 63, no. 10, pp. 4529–4534, Oct. 2015.
[36] R. Azim, A. T. Mobashsher, and M. T. Islam, "UWB antenna with notched band at 5.5 GHz," *Electron. Lett.*, vol. 49, no. 15, pp. 922–924, Jul. 2013.
[37] M. S. Ellis, Z. Zhao, J. Wu, Z. Nie, and Q. Liu, "A novel miniature band-notched wing-shaped monopole ultrawideband antenna," *IEEE Antennas Wireless Propag. Lett.*, vol. 12, pp. 1614–1617, 2013.
[38] Y. F. Wang, T. A. Denidni, Q. S. Zeng, and G. Wei, "Band-notched UWB rectangular dielectric resonator antenna," *Electron. Lett.*, vol. 50, no. 7, pp. 483–484, Mar. 2014.
[39] P. Gao, L. Xiong, and J. B. Dai, "Compact printed wide-slot UWB antenna with 3.5/5.5-GHz dual band-notched characteristics," *IEEE Antennas Wireless Propag. Lett.*, vol. 12, pp. 983–986, 2013.
[40] M. B. Knudsen and G. F. Pedersen, "Spherical outdoor to indoor power spectrum model at the mobile terminal," *IEEE J. Sel. Areas Commun.*, vol. 20, no. 6, pp. 1156–1168, Aug. 2002.
[41] M. S. Khan, A. Capobianco, A. I. Najam, I. Shoaib, E. Autizi, and M. F. Shafique, "Compact ultra-wideband diversity antenna with a floating parasitic digitated decoupling structure," *IET Microw., Antennas Propag.*, vol. 8, no. 10, pp. 747–753, Jul. 2014.
[42] R. Tian, B. K. Lau, and Z. Ying, "Multiplexing efficiency of MIMO antennas," *IEEE Antennas Wireless Propag. Lett.*, vol. 10, pp. 183–186, 2011.

ZHIJUN TANG received the B.S., M.S., and Ph.D. degrees in electrical engineering from Hunan University, Changsha, China, in 1998, 2003, and 2010, respectively.

From 2003 to 2009, he was a Lecturer. From 2010 to 2015, he was an Associate Professor with the Communication Engineering Department, Hunan University of Science and Technology, Xiangtan, China, where he has been a Professor, since 2016. Since 2019, he has been with the School of Electronic Information and Electrical Engineering, Changsha University, Changsha. He has authored over 40 research papers. His main research interests include UWB-MIMO antenna design, RFID electromagnetic modeling and antenna design, and photoelectric information function devices.

Dr. Tang has received several grants, in recent years, from the National Natural Science Foundation of China. He is an Invited Reviewer for many international journals in the field of microwave, antenna, and optics.

XIAOFENG WU received the B.S. degree in industrial automation from the Hunan University of Science and Technology, Xiangtan, China, in 1998, the M.S. degree in industrial automation from Hunan University, Changsha, China, in 2003, and the Ph.D. degree in microelectronics from Xidian University, Xi'an, China, in 2010.

From 2003 to 2009, he was a Lecturer. From 2010 to 2015, he was an Associate Professor with the Electronic Information Engineering Department, Hunan University of Science and Technology, Xiangtan, China, where he has been a Professor, since 2016. He has authored over 50 articles. His research interests include the semiconductor devices, functional materials, upconversion nanopartical synthesis and application, and biosensors.

JIE ZHAN received the B.S. degree in physics from the Hunan University of Science and Technology, Xiangtan, China, in 1995, and the M.S. and Ph.D. degrees in circuit and system from Hunan University, Changsha, China, in 2008 and 2011, respectively. Since 2017, he has been a Professor with the Physics Department, Hunan University of Science and Technology. His research interests include wireless communication, senor networks, and UWB antenna technology.

SHIGANG HU received the B.S. degree in electronic information engineering from the Hubei University of Technology, Wuhan, China, in 2003, and the Ph.D. degree in microelectronics from Xidian University, Xi'an, China, in 2009. Since 2013, he has been an Associate Professor with the Electronic Information Engineering Department, Hunan University of Science and Technology, Xiangtan, China. His research interests include semi-conductor devices, functional materials, and upconversion nanopartical synthesis and application.

ZAIFANG XI received the B.S. degree in electronic information engineering from Xiangtan University, Xiangtan, China, in 1996, and the M.S. degree in circuit and system from Hunan University, Changsha, China, in 2003. Since 2009, he has been an Associate Professor with the Communication Engineering Department, Hunan University of Science and Technology, Xiangtan. His research interests include signal processing and wireless communication technology.

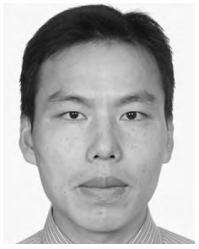

YUNXIN LIU received the B.S. degree in physics and the Ph.D. degree in materials physics and chemistry from Xiangtan University, Xiangtan, China, in 2004 and 2009, respectively.

From 2009 to 2012, he was a Lecturer with the Physics Department, Hunan University of Science and Technology, Xiangtan, China, where he has been an Associate Professor, since 2013. He held a Postdoctoral position with Tsinghua University, Beijing, China, from 2010 to 2013. He was a Visiting Scholar with the Catholic University of Louvain, Louvain, Belgium, from 2014 to 2015. He has authored over 50 articles. He holds two patents. His research interests include the rare earth upconversion nanomaterials, optomagnetic materials, biosensors, and plasmon-enhanced upconversion. He is an Invited Reviewer of the *Journal of Materials Chemistry C* and the *Journal of Applied Physics*.